

Run08pp Central Arm EMC ToF Calibration

John Koster^a, Mickey Chiu^b, Matthias Große Perdekamp^a

^a University of Illinois at Urbana Champaign

^b Brookhaven National Laboratory

Abstract

A calibration of the central arm time of flight is presented. The ToF cut which this calibration enables reduces the possibility of a feature in the central arm calorimeter electronics to produce spin-dependent effects and improves the signal background ratio for π^0 and η meson's.

Contents

1	Introduction	1
2	Analysis	1
2.1	CVS Location of Code	1
2.2	Overview	1
2.3	0.3 GeV analysis	2
2.4	1.0 GeV analysis	4
2.5	Discussion	6
2.6	Results	6
2.7	Investigation of ToF1 \approx ToF2	12
3	Appendix: Bad tower list	17
3.1	Variance check	17
3.2	Unstable values	17

1 Introduction

The central arm electromagnetic calorimeter is divided into eight sectors. Six of the eight sectors are lead scintillator sampling calorimeters (PbSc) and the remaining sectors are lead glass (PbGl). Each PbSc sector is composed of a 36 (y) x 72 (z) grid of towers while each PbGl sector is composed of a 48 (y) x 96 (z) grid of towers. Towers can be uniquely referenced given a sector identifier and the gridy/gridz position, or with a global tower identifier. This analysis makes use of the global tower identifier to minimize the total number of plots.

Each tower in the calorimeter has a constant timing offset which needs to be determined and subtracted before a time of flight can be applied. This note describes the measurement of this offset for run8.

2 Analysis

2.1 CVS Location of Code

The code used in this analysis is available at:

`offline/analysis/koster/EmcTof`

2.2 Overview

Run by run and tower by tower timing histograms are generated with a set of cuts which should select a photon sample (or at least suppress hadrons) from ERT triggered events. The cuts are:

- **PHGlobal::getBbcZVertex()** zvertex of the collision. Events outside of $\pm 30\text{cm}$ are removed from analysis. This is a standard offline analysis cut in the central arm.
- **emcClusterContent::ecore()** applies a cluster energy cut.
- **emcClusterContent::prob_photon() >0.02** Selects showers which are consistent with an electromagnetic shower
- **Warnmap veto** Towers which are already flagged as bad [1] are removed from the analysis

For all the clusters passing these cuts, I find the tower center of the cluster (`emcClusterContent::towerid(0)`). Then, I fill a tower by tower histogram of time of flight (`emcClusterContent::tof() - PHGlobal::get_BbcTimeZero()`). I fill the histograms using a 0.3 and a 1.0 GeV cluster energy cut. The offset value is taken as the bin with the largest content. The distributions of ToF and ToF-t0 are aggregated over all of run8pp and plotted in figures 1 and 2 with the low and high energy cut.

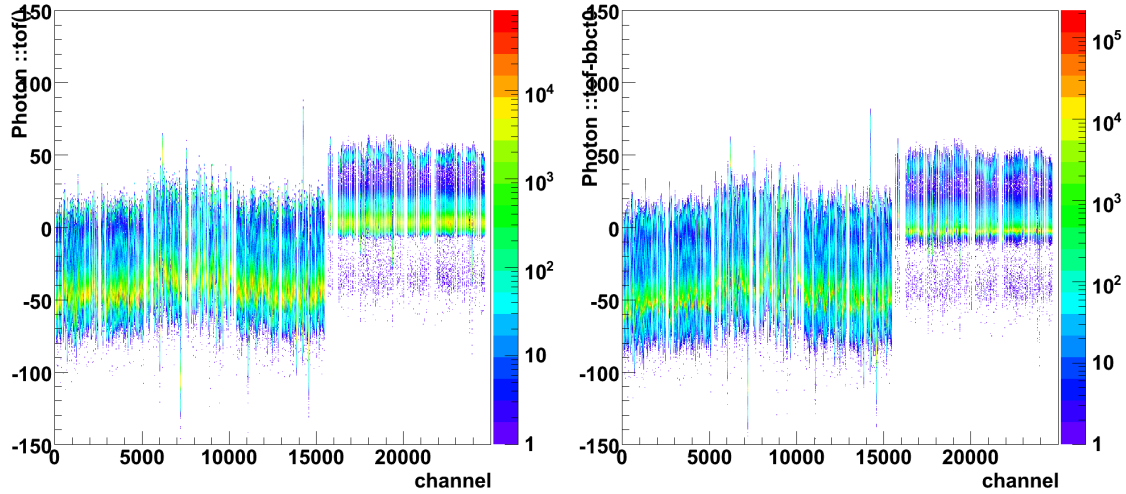


Figure 1: Xaxis: EMC tower number, Yaxis: `emcClusterContent::tof()` (left), `emcClusterContent::tof()-PHGlobal::get_BbcTimeZero()` (right). The distributions tighten up noticeably with the subtraction of the start time. The minimum cluster energy is 0.3 GeV.

The 300 MeV energy cut gives sufficient statistics to perform the offset analysis on a run by run basis which is then checked for stability over runnumber. The values are found to be stable for all but 200 towers. In at least one of these bad towers the offset value fluctuated between two peaks of nearly equal size. This

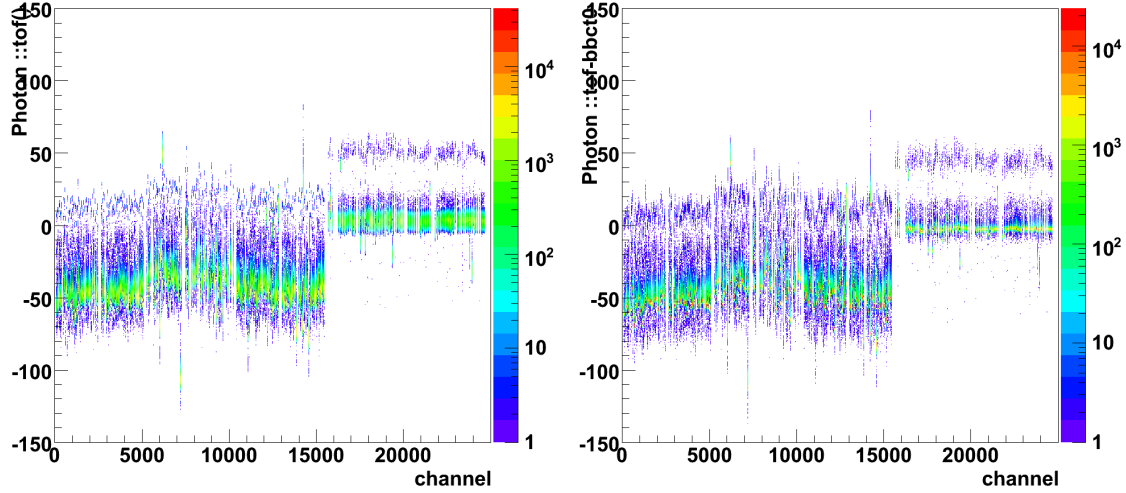


Figure 2: Xaxis: EMC tower number, Yaxis: `emcClusterContent::tof()` (left), `emcClusterContent::tof()-PHGlobal::get_BbcTimeZero()` (right). The distributions tighten up noticeably with the subtraction of the start time. The minimum cluster energy is 1.0 GeV

suggests that there were two peaks: one photonic and the other from tdc timeout. It also raises the possibility that in other towers there is a larger timeout peak than a photonic peak. Therefore, the analysis is repeated using a 1 GeV energy cut. There aren't sufficient statistics to do the analysis run by run, but the offsets can be derived by aggregating over all of run8pp. Comparison between figures 1 and 2 shows that the the higher energy cut greatly reduces the smaller second peak at higher time values compared to the dominant peak at low time. The low time peak is therefore assumed to be photonic in origin.

2.3 0.3 GeV analysis

For each run and each tower the offset is determined by finding the bin with the highest number of counts. For each tower the variance of the offset is determined over all run8pp runs. The variance for each tower is shown in figure 3. If the variance is greater than two nanoseconds², the tower is flagged as a bad tower. These towers are listed in section: 3. A random sample of the bad towers was investigated by aggregating the timing distribution from all runs, and looking at individual towers. Examples of good and bad towers are provided in figures 4 and 5.

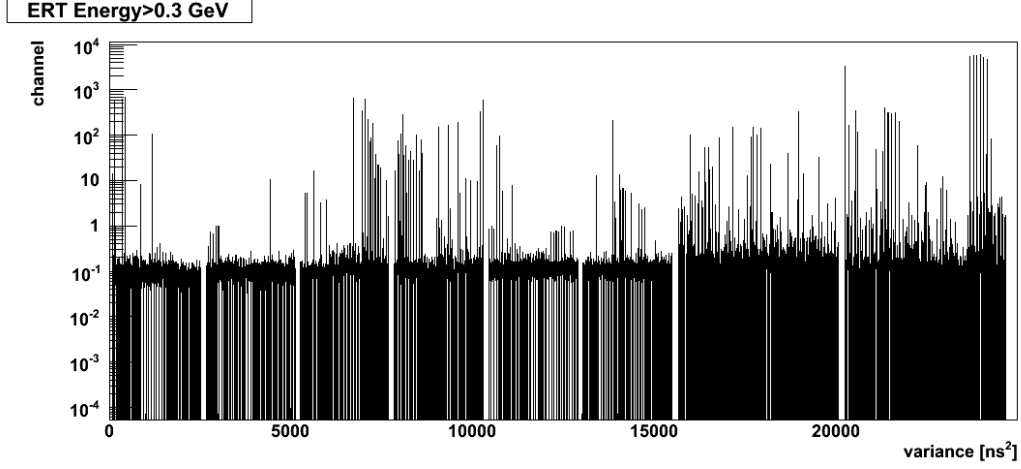


Figure 3: Yaxis: offset variance (described in text), Xaxis: EMC tower number. Minimum cluster cut: 300 MeV

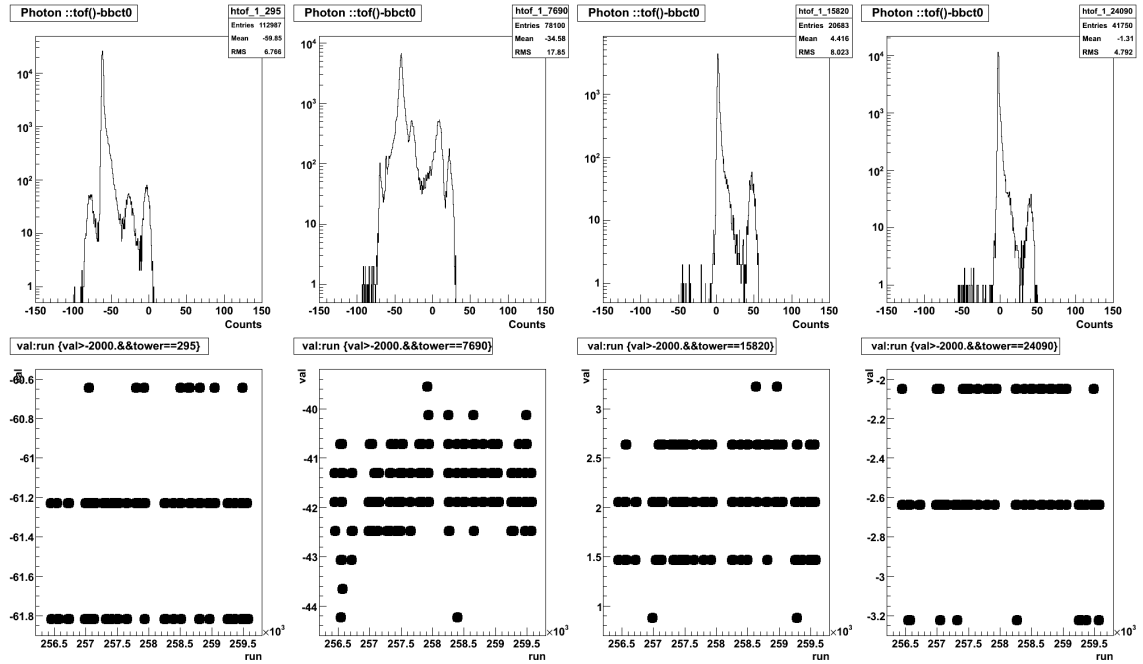


Figure 4: A selection of four random towers which are marked as good towers. Top: timing distributions, Bottom: Offset value plotted against runnumber.

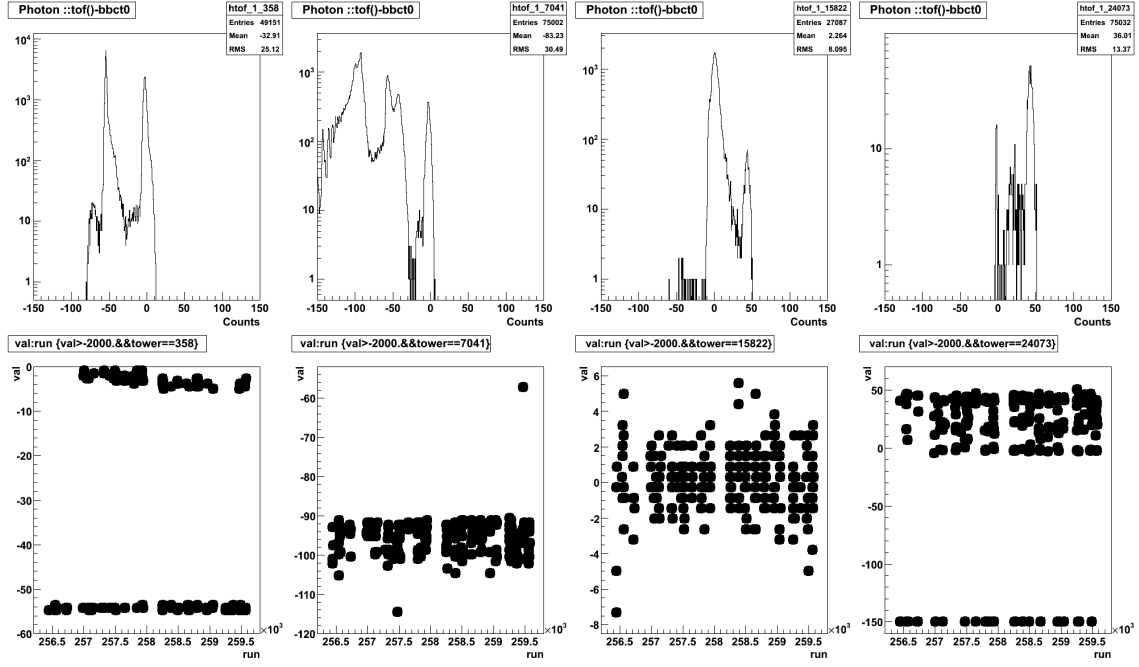


Figure 5: A selection of four random towers which are marked as bad towers. Top: timing distributions, Bottom: Offset value plotted against runnumber.

2.4 1.0 GeV analysis

To reduce the possibility of mis-identifying the two peaks, the analysis from the previous section is repeated with a 1 GeV instead of a 0.3 GeV cluster energy cut. The histograms are aggregated over all run numbers, and the bin with the maximum population is found for each tower's ToF distribution. This maximum bin offset is taken as the final offset result.

2.5 Discussion

The offset values from the 0.3 and 1.0 GeV analysis are plotted and compared in figure 6. Towers with a difference between the 0.3 and 1.0 GeV analyses greater than 5 nanoseconds are listed in section 3.

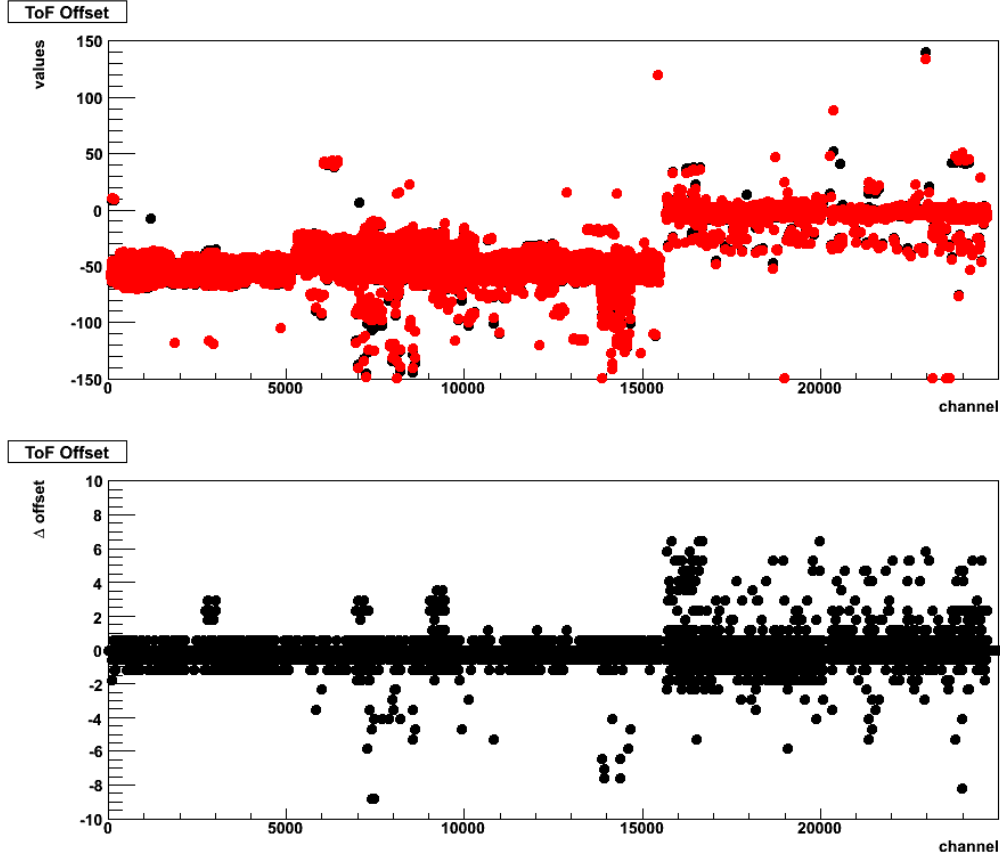


Figure 6: Xaxis: channel. Top panel Yaxis: offset value (black 0.3 GeV cut, red 1.0 GeV cut), Bottom panel Yaxis: Difference between 0.3 and 1.0 GeV offset values. The range for the bottom panel is fixed to lie between ± 10 nanoseconds. Towers with a difference greater than 5ns are listed in text and removed from analysis.

2.6 Results

The results of the calibration are in a root file available at:

<http://www.phenix.bnl.gov/WWW/publish/jkoster4/note/TNTToF/>

The time of flight distribution ¹ aggregated over all towers and all of run8pp is shown in figures 7 and 8. The following cuts enhance the photon sample:

¹emcClusterContent::tof()-PHGlobal::getBbcTimeZero()-ToF_Offset[tower]

- **Warnmap veto:** The warnmap is the super set of the bad towers from this calibration and Kenichi's warnmap
- **Minimum energy:** `emcClusterContent::ecore()` > 0.2. A 200 MeV cut on cluster energy
- **Shower shape:** `emcClusterContent::prob_photon()` > 0.02.

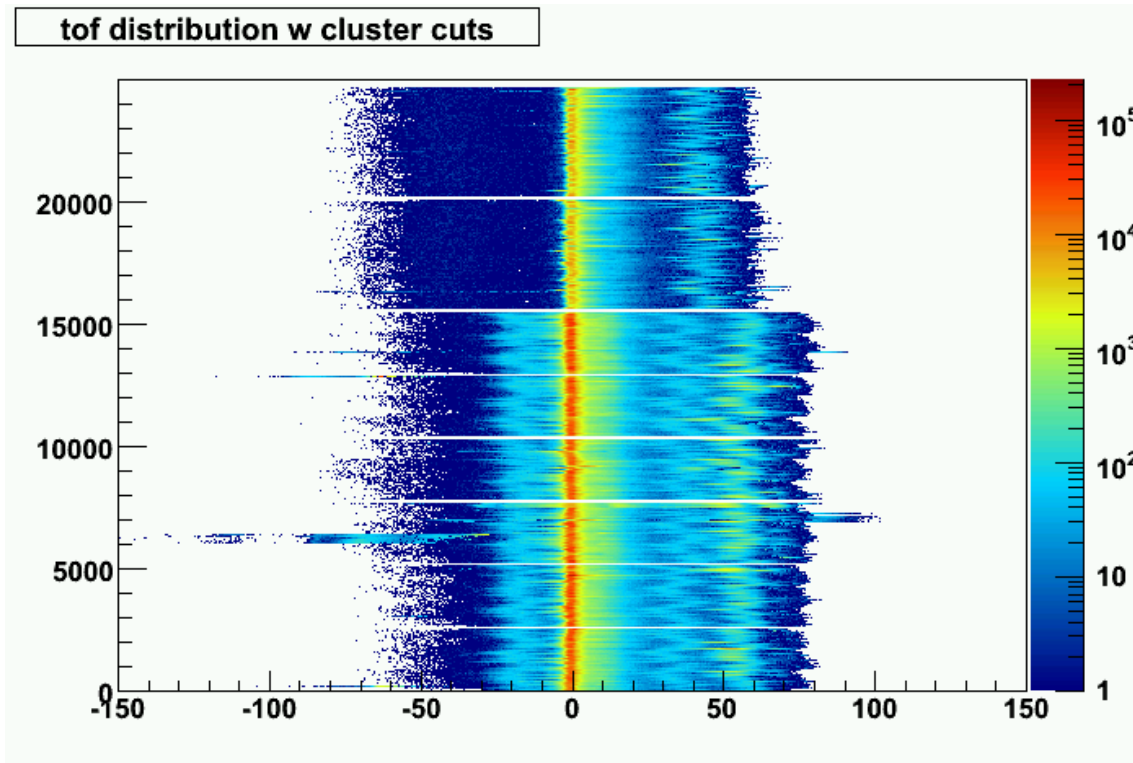


Figure 7: Xaxis: channel, Yaxis: ToF [ns], Zaxis: counts. Trigger: ERT4x4A or ERT4x4C.

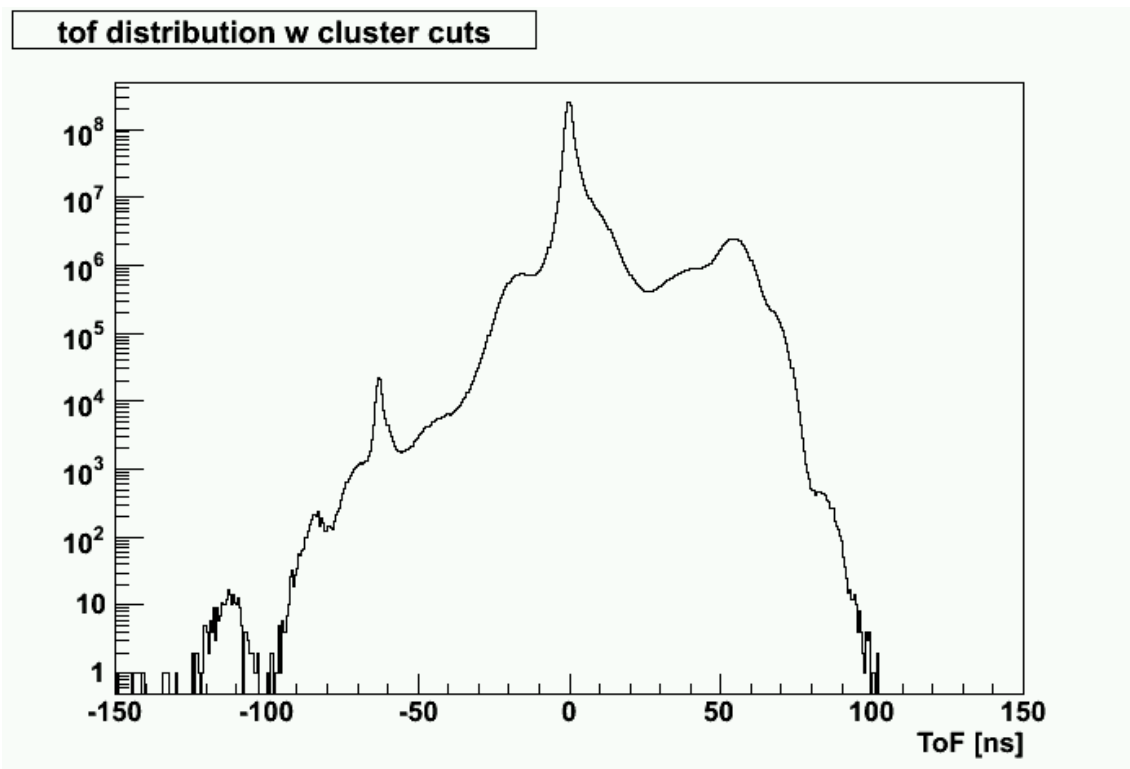


Figure 8: Xaxis: ToF [ns], Yaxis: counts. Same as figure 7 but projected to show only the ToF. Trigger: ERT4x4A or ERT4x4C.

As a further check of the calibration, pairs are formed between clusters from the same event using the following criteria:

- **Energy Asymmetry:** must be less than 0.8
- **Active Supermodule:** If the trigger is an ERT trigger, the higher energy cluster must have an active trigger bit in its supermodule.

The correlation between the ToF of each cluster making up a pair is shown in figures 9 and 10 for ERT and minimum bias triggered data respectively. There are several structures in the correlation. By construction the counts at zero time of flight are photons while hadrons arrive distributed over times later than zero. When pairs are formed four combinations are possible: γ, γ ; γ, h ; h, γ ; h, h . These four combinations lead to the cross like structure centered at (0,0). In addition to the horizontal and vertical correlations, figure 9 shows correlation along $\text{tof1} \approx \text{tof2}$. I can't claim to understand this correlation very well, but these pairs do not give a large contribution on the π^0 mass peak. See figure 11 to see the tof correlation plot for pairs with a mass between 100 and 160 MeV.

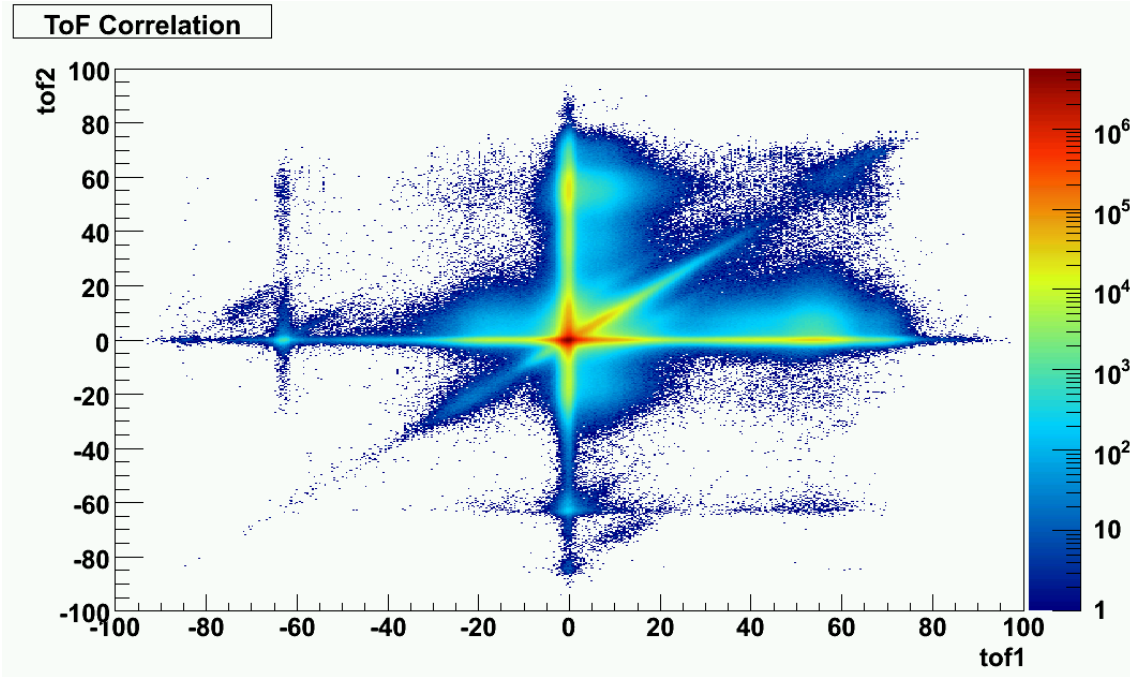


Figure 9: X,Y axis: time of flight for clusters, Z axis: counts. Trigger: ERT4x4A or ERT4x4C. Plot is aggregated over all of run8pp.

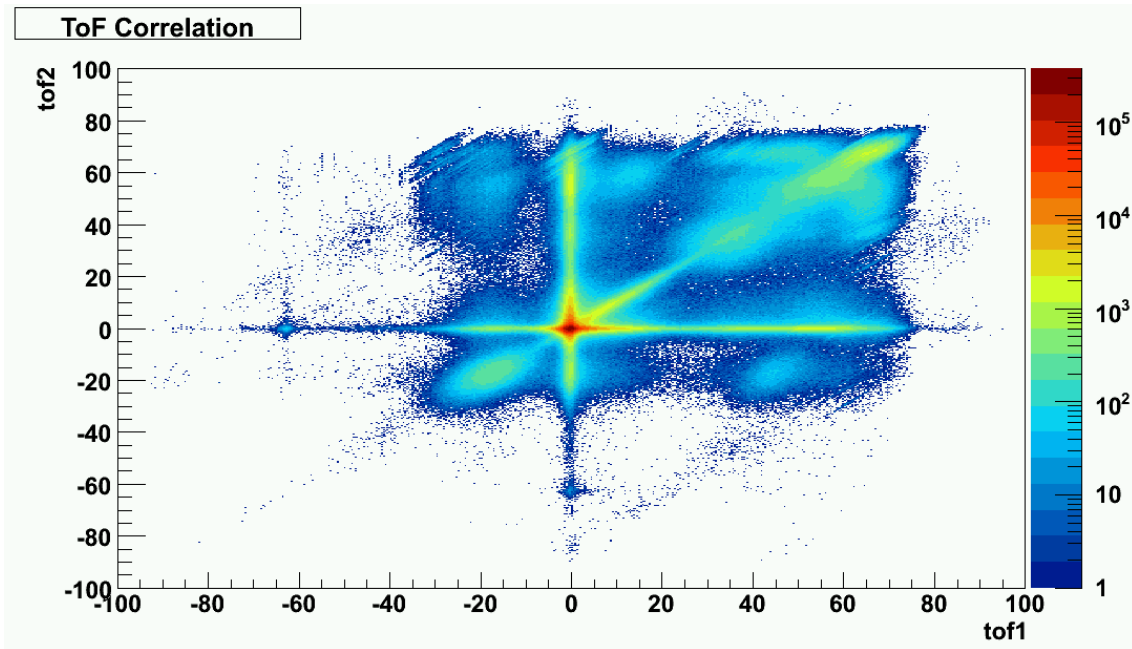


Figure 10: X,Y axis: time of flight for clusters, Z axis: counts. Trigger: Minimum bias. Plot is aggregated over all of run8pp.

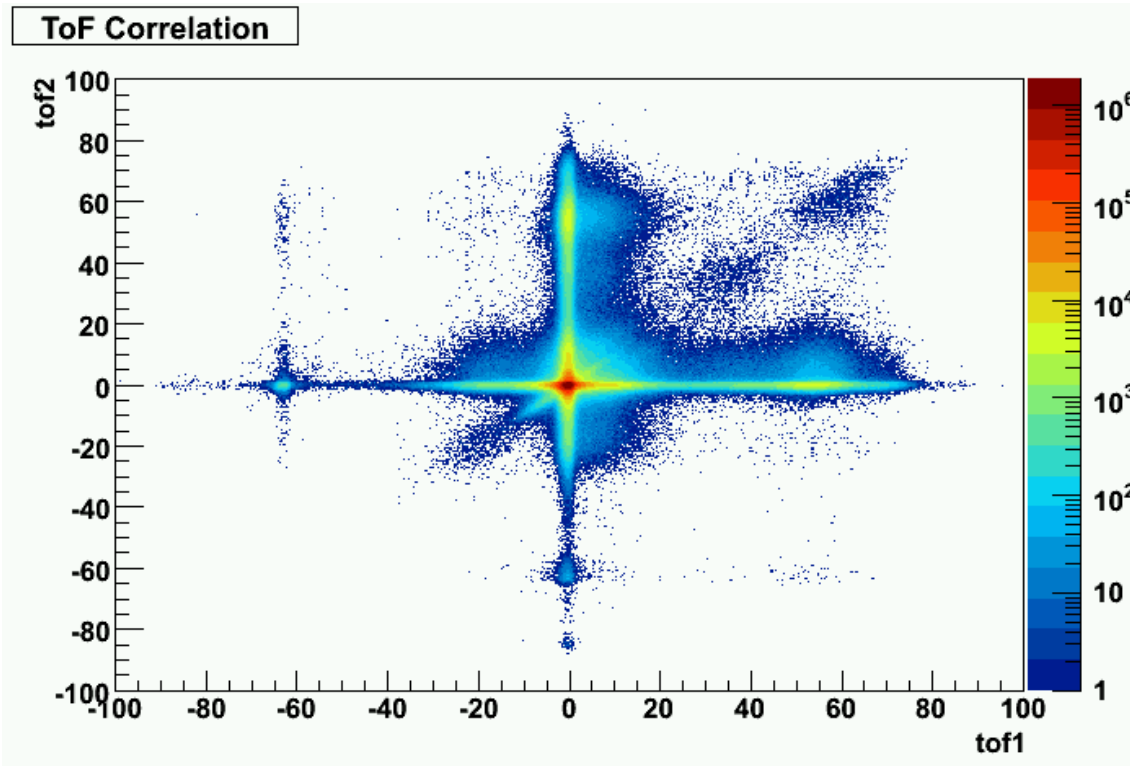


Figure 11: X,Y axis: time of flight for clusters, Z axis: counts. Trigger: ERT4x4A or ERT4x4C. The pair mass is required to lie between 100 and 160 meV. Plot is aggregated over all of run8pp.

2.7 Investigation of $\text{ToF1} \approx \text{ToF2}$

I talked to several people about the ToF correlations. Here are the theories we came up with:

1. Bad t_0 (discussion w/ Kensuke). If the t_0 is badly measured, two photons will arrive at the same time but not at zero ToF. The t_0 hypothesis is disproven by figure 14.
2. Conversions (Mickey). Would expect low pair mass.
3. Low momenta charged hadrons with large incidence angles (created by the magnetic field) which shower in the EMC but are reconstructed as two separate clusters (Kieran's hypothesis).

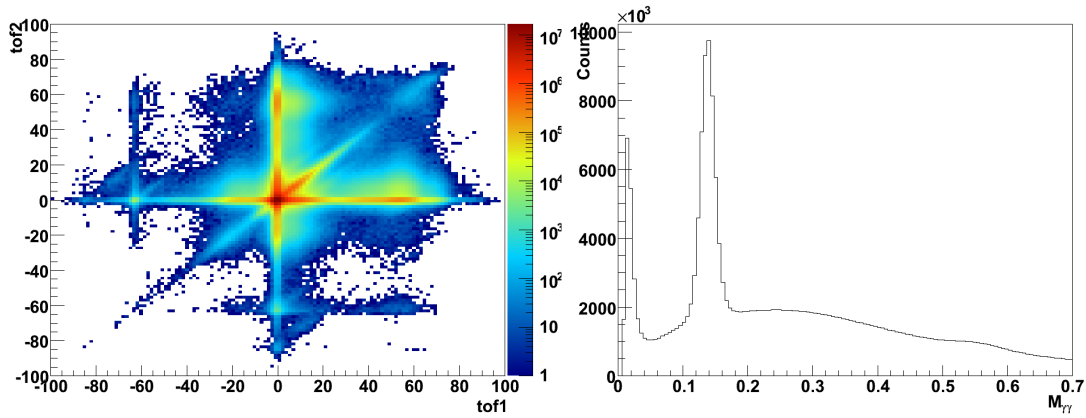


Figure 12: Left: X/Y axis time of flight for clusters, Z axis counts; Right: di cluster invariant mass distribution. Trigger: ERT4x4A or ERT4x4C. Inclusive ToF selection.

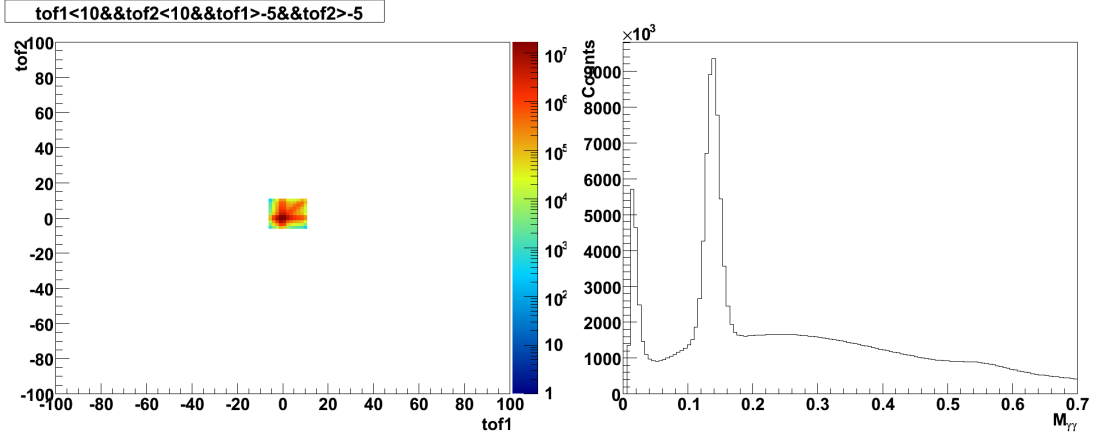


Figure 13: Left: X/Y axis time of flight for clusters, Z axis counts; Right: di cluster invariant mass distribution. Trigger: ERT4x4A or ERT4x4C. $-5 < ToF_{1,2} < 10$

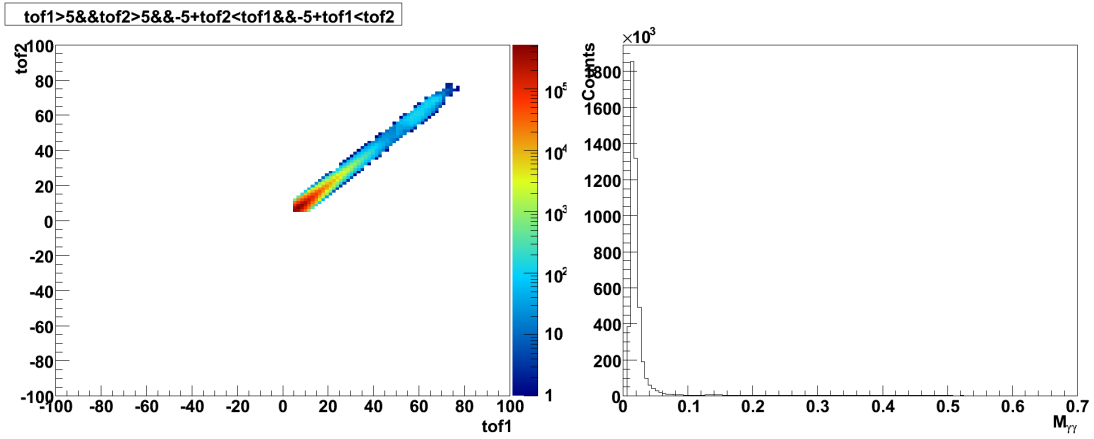


Figure 14: Left: X/Y axis time of flight for clusters, Z axis counts; Right: di cluster invariant mass distribution. Trigger: ERT4x4A or ERT4x4C. The ToF's were cut to select the correlated ToF region. The exact selection can be seen in the left panel.

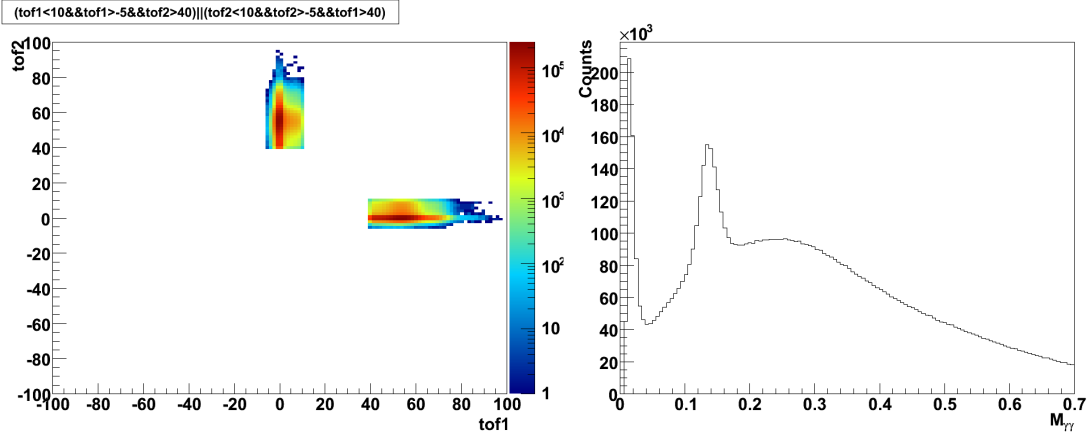


Figure 15: Left: X/Y axis time of flight for clusters, Z axis counts; Right: di cluster invariant mass distribution. Trigger: ERT4x4A or ERT4x4C. The ToF's were cut to select photon+hadron pairings. The exact selection can be seen in the left panel.

Figure 16 shows the four mass distributions drawn on one canvas to give a sense of their relative contributions to the inclusive di-photon mass spectra. It shows that the low mass spike at around 5 MeV receives a large contribution from the crude ToF selection shown in figure 14. The source of the low mass

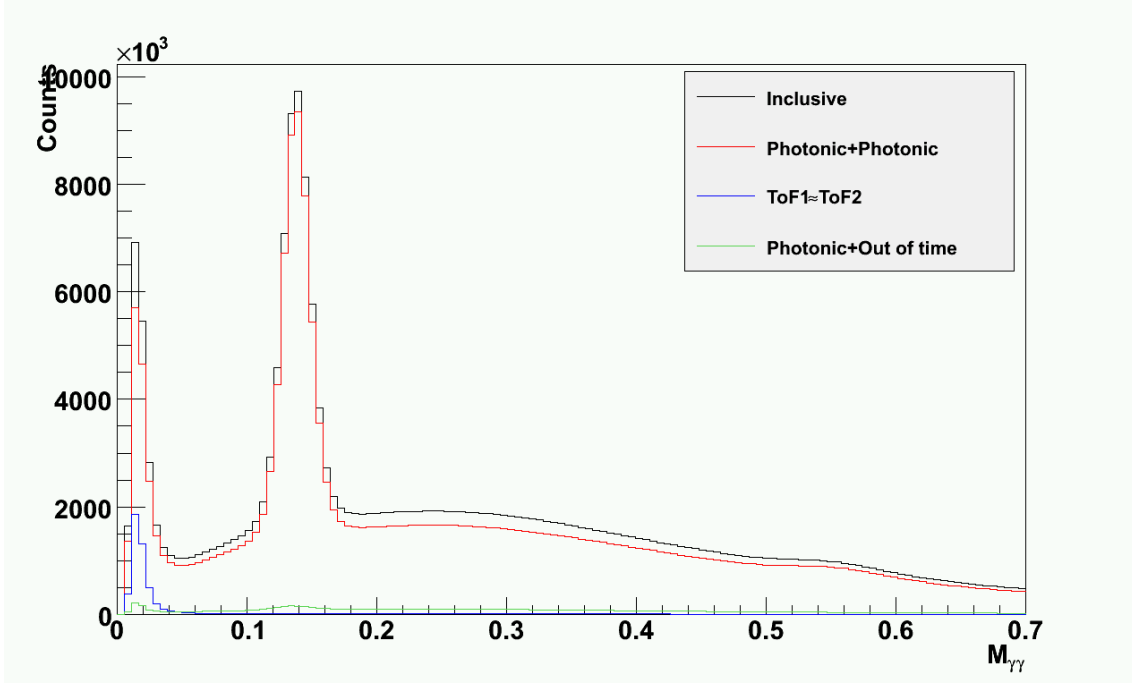


Figure 16: Xaxis: dicluster invariant mass; Yaxis: counts. Tof selections for black, red, blue and green show in figures 12,13,14,15

distribution is further explored by taking the tof correlation from 14 and dividing it by the inclusivetoF correlation (figure 12). The zaxis of the resulting histogram shown in figure 17 shows that the yields at low mass are dominated by their contribution along the tof1 \approx tof2 correlation.

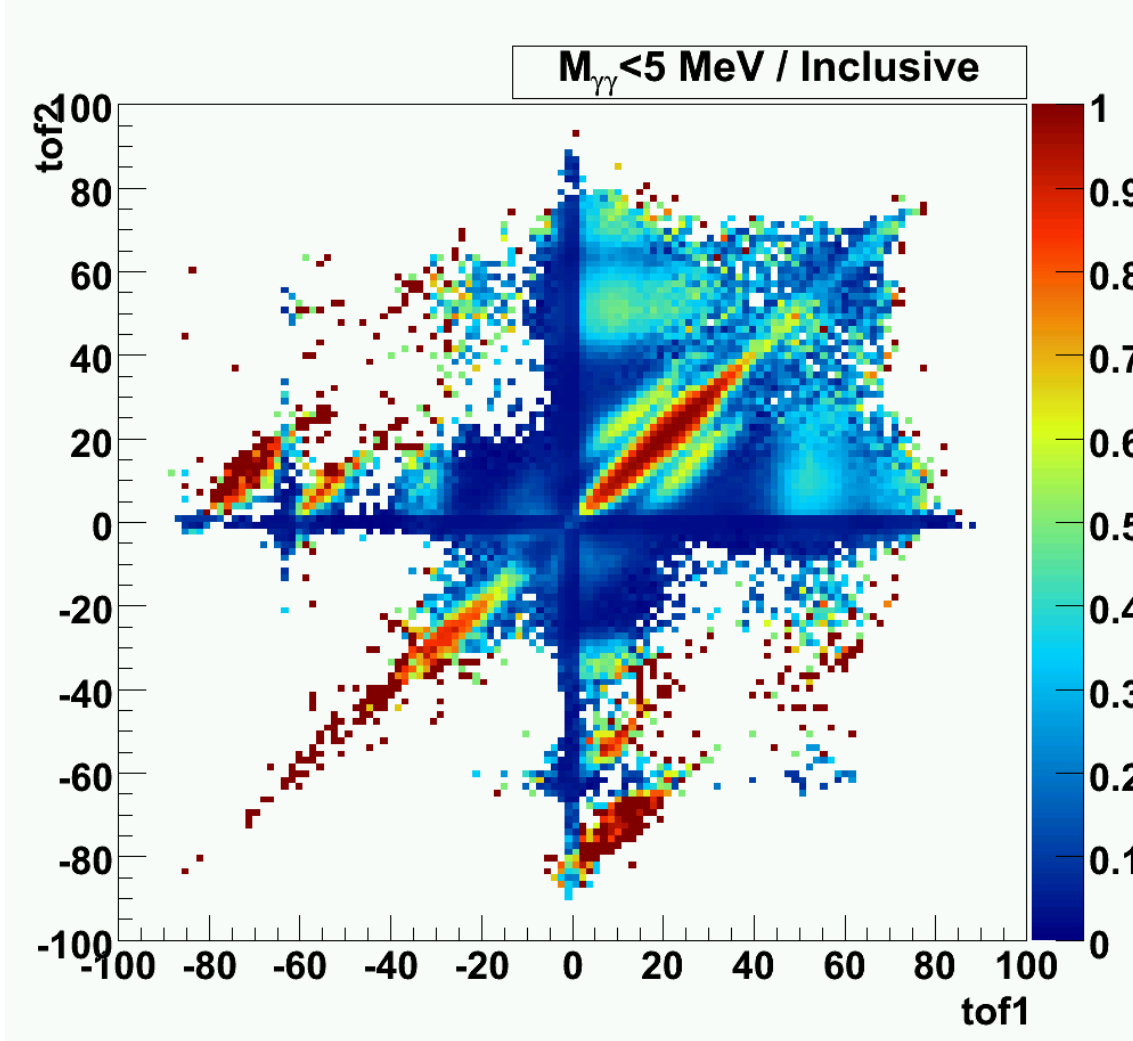


Figure 17: X/Yaxis: tof of clusters. Zaxis yield of pairs with mass less than 5 MeV divided by the yields without a mass cut.

References

- [1] K. Nakano, https://www.phenix.bnl.gov/WWW/p/draft/kenichi/emcal/energy_calib_run8/

3 Appendix: Bad tower list

Lists of the bad towers in the global identifier (.fee) and in sector, gridy, gridz (.syz) are provided here:

<https://www.phenix.bnl.gov/WWW/publish/jkoster4/note/TNTToF/>

3.1 Variance check

Towers whose time offset variance over runnumber is greater than 2 ns^2 from the 0.3 GeV cluster energy cut analysis are flagged as bad towers.

92 142 358 430 862 1173 4431 5376 5449 5636 5824 5969 6710 6967 6968 6969
6970 7035 7039 7040 7041 7042 7111 7112 7113 7115 7179 7183 7185 7186 7250
7255 7256 7257 7310 7328 7329 7380 7382 7398 7452 7453 7474 7615 7869 7940
7964 8012 8013 8071 8075 8085 8108 8109 8157 8180 8229 8300 8373 8445 8540
8541 8588 8589 8613 9075 9323 9371 9595 9642 9815 9938 10141 10212 10284
10667 10668 10669 10734 10740 10741 10809 11091 13393 13851 13922 14038
14066 14138 14211 14371 14374 14375 14586 14587 14663 14728 14729 15679
15742 15770 15822 15838 15986 16033 16129 16206 16207 16222 16225 16302
16321 16341 16398 16399 16414 16494 16495 16499 16510 16590 16591 16606
16686 16687 16790 17047 17156 17312 17555 17651 17661 17725 17816 17831
17922 18188 18198 18674 18686 18945 18967 18979 19095 19544 19772 19973
19987 20257 20353 20446 20527 20541 20606 20830 20961 21117 21118 21233
21296 21342 21343 21365 21438 21439 21534 21630 21735 22020 22262 22455
22457 22498 22886 22942 23038 23689 23690 23708 23709 23765 23785 23804
23805 23806 23881 23900 23901 23972 23976 23977 23996 23997 24072 24073
24092 24093 24146 24147 24168 24169 24188 24220 24271 24284 24289 24461
24476 24481 24525 24577

3.2 Unstable values

Towers whose offset values differ by more than 5 nanoseconds between the 0.3 and 1.0 GeV analyses are added to the bad tower list:

1174 5747 5748 7043 7258 7381 7454 8086 8109 8158 8446 8542 10810 12857
13867 13923 13935 14372 14375 14376 14587 14588 15680 15823 15919 16034
16112 16342 16400 16508 16514 16533 16591 16687 16688 17662 17923 18675
18946 18968 19081 19773 19988 20258 20298 20354 20542 20607 21344 22021
22458 22496 22943 23039 23690 23786 23978 24074 24169 24255 24526